Organic Single-Crystal Field-Effect Transistors of a Soluble Anthradithiophene

Oana D. Jurchescu,*,†,‡ Sankar Subramanian,§ R. Joseph Kline,|| Steven D. Hudson,|| John E. Anthony,§ Thomas N. Jackson,‡ and David J. Gundlach*,†

Semiconductor Electronics Division and Polymers Division, National Institute of Standards and Technology, Gaithersburg, Maryland, Center for Thin Film Devices and Materials Research Institute, Department of Electrical Engineering, Penn State University, University Park, Pennsylania, and Department of Chemistry, University of Kentucky, Lexington, Kentucky

Received August 1, 2008. Revised Manuscript Received September 5, 2008

We present the first characterization of single-crystal devices of a new solution processable material that we have previously demonstrated achieves technologically relevant performance in the polycrystalline thin film state. Our studies include growth and investigation of structural, as well as electronic properties of single crystals of 2,8-difluoro-5,11-bis(triethylsilylethynyl) anthradithiophene (diF-TESADT). Field-effect transistors fabricated on the surface of diF-TESADT single crystals exhibit excellent electronic properties: mobility as high as 6 cm^2/Vs, large current on/off ratios ($I_{on}/I_{off} = 1 \times 10^8$), small subthreshold slopes ($S = 1$ V/dec), and extremely small hysteresis in the current−voltage characteristics. These properties, coupled with solution processability, make diF-TESADT attractive for electronic applications and demonstrate the technological potential of soluble oligomers.

Introduction

Organic semiconductors are of scientific and technological interest because of their electrical properties and potential use in low-cost large-area electronic applications. Oligomers, such as pentacene and rubrene, are particularly attractive given the high mobilities reported.[1,2] However, a significant drawback of most high-performance oligomers is their limited solubility, or poor film forming properties when deposited from solution, which makes them incompatible with low-cost solution deposition methods.[3,4] This deficiency has motivated an intense effort to chemically tailor the molecular properties of organic semiconductors to increase their solubility and achieve ease of processing while maintaining or improving the device performance.

One approach is the attachment of halogens[5] or flexible side groups[6] to conventional small molecule semiconductors. This approach can also promote cofacial packing of the molecules, which accommodates the largest π overlap and is believed to be beneficial for charge transport.[7] Time-resolved terahertz pulse spectroscopy was recently used to demonstrate similar transient photoconductivities in pentacene and the soluble homologue 6,13-bis(triisopropyl-silylethynyl) pentacene (TIPS-pentacene) over picosecond timescales (nanometer length-scales).[8] But thus far, the macroscopic electrical properties of devices fabricated by using soluble oligomers have not reached the performance benchmarks set by devices fabricated from single crystals of pentacene or rubrene, for which mobilities on the order of 1×10 cm^2/(V s) were measured.[1−3,9,10] For example, mobilities of 1.2 cm^2/(V s) were achieved in films fabricated by drop-casting TIPS-pentacene from toluene solution,[11] and 1.42 cm^2/(V s) in single-crystalline microribbons of the same material obtained via the solvent-exchange method.[12] For the class of anthradithiophenes, mobilities of 0.1 cm^2/(V s) were obtained in 5,11- bis(triethylsilylethynyl) anthradithiophene (TES ADT) films upon solvent annealing,[13] and 1 cm^2/(V s) in slow-dried films.[14] In fluorinated 5,11-bis(triethylsilylethynyl) anthradithiophene (diF-TES ADT), a mobility

* To whom correspondence should be addressed. E-mail: oana.jurchescu@nist.gov (O.D.J.); david.gundlach@nist.gov (D.J.G.).
† Semiconductor Electronics Division, National Institute of Standards and Technolog.
‡ Penn State University.
§ University of Kentucky.
|| Polymers Division, National Institute of Standards and Technology.

(1) Sundar, V. C.; Zaumseil, J.; Podzorov, V.; Menard, E.; Willett, R. L.; Someya, T.; Gershenson, M. E.; Rogers, J. A. *Science* **2004**, *303*, 1644.
(2) Jurchescu, O. D.; Popinciuc, M.; van Wees, B. J.; Palstra, T. T. M. *Adv. Mater.* **2007**, *19*, 688.
(3) Gershenson, M. E.; Podzorov, V.; Morpurgo, A. F. *Rev. Mod. Phys.* **2006**, *78*, 973.
(4) Mas-Torrent, M.; Durkut, M.; Hadley, P.; Ribas, X.; Rovira, C. *J. Am. Chem. Soc.* **2004**, *126*, 984.
(5) Moon, H.; Zeis, R.; Borkent, E.-J.; Besnard, C.; Lovinger, A. J.; Siegrist, T.; Kloc, C.; Bao, Z. *J. Am. Chem. Soc.* **2004**, *126*, 15322.
(6) Anthony, J. E.; Eaton, D. L.; Parkin, S. *Org. Lett.* **2002**, *4*, 15.
(7) Bredas, J.-L.; Beljonne, D.; Coropceanu, V.; Cornil, J. *Chem. Rev.* **2004**, *104*, 4971.
(8) Ostroverkhova, O.; Cooke, D. G.; Hegmann, F. A.; Anthony, J. E.; Podzorov, V.; Gershenson, M. E.; Jurchescu, O. D.; Palstra, T. T. M. *Appl. Phys. Lett.* **2006**, *88*, 162101.
(9) Briseno, A. L.; Mannsfeld, S. C. B.; Ling, M. M.; Liu, S.; Tseng, R. J.; Reese, C.; Roberts, M. E.; Yang, Y.; Wudl, F.; Bao, Z. *Nature* **2006**, *444*, 913.
(10) Goldmann, C.; Krellner, C.; Pernstich, K. P.; Haas, S.; Gundlach, D. J.; Batlogg, B. *J. Appl. Phys.* **2006**, *99034507*, 2006.
(11) Park, S.; Jackson, T. N.; Anthony, J. E.; Mourey, D. A. *Appl. Phys. Lett.* **2007**, *91*, 063514.
(12) Kim, D. H.; Lee, D. Y.; Lee, H. S.; Lee, W. H.; Kim, Y. H.; In Han, J.; Cho, K. *Adv. Mater.* **2007**, *19*, 678.
(13) Dickey, K. C.; Anthony, J. E.; Loo, Y.-L. *Adv. Mater.* **2006**, *18*, 1721.
(14) Payne, M. M.; Parkin, S. R.; Anthony, J. E.; Kuo, C.-C.; Jackson, T. N. *J. Am. Chem. Soc.* **2005**, *127*, 4986.

10.1021/cm8021165 CCC: $40.75
Published on Web 10/22/2008

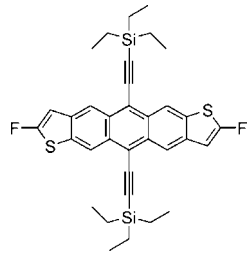

Figure 1. Chemical formula of the diF-TES ADT molecule.

of 0.2 $cm^2/(Vs)$ was measured for films spin-coated from toluene,[15] and 0.4 $cm^2/(V\ s)$ for the films spin-coated from a solution in chlorobenzene.[16] Reviewing these different values for the mobility in devices fabricated by different processing methods, it is obvious that they are influenced by many factors. The question is whether the relatively low values of mobilities come from an intrinsic limitation, related to the molecular packing, or are related to thin film imperfections (grain-boundaries, solvent-related effects, microstructure, polymorphs, etc).

To address this question, we investigate a soluble material that we have previously reported to reach high device performance in the polycrystalline thin film form,[15,16] and evaluate the intrinsic properties by measuring single crystals. This approach allows a better understanding of the intrinsic properties, limitations, and potential of these materials. Single crystals (here grown by physical vapor transport) are well-suited for studies exploring the effects of chemical structure and molecular packing separate from thin film effects. We report on the fabrication of organic field-effect transistors from 2,8-difluoro-5,11-bis(triethylsilylethynyl) anthradithiophene (diF-TESADT) single crystals (see chemical structure in Figure 1). In brief, the general characteristics of these devices are high mobilities ($\mu_{max} = 6\ cm^2/(V\ s)$), large current on/off ratios ($I_{on}/I_{off} \approx 1 \times 10^8$), small subthreshold slopes ($S \approx 1$ V/dec) and extremely small hysteresis in the current−voltage characteristics, demonstrating that remarkable intrinsic properties are possible from these soluble variants. To the best of our knowledge, this is the first time that a soluble oligomer organic semiconductor with demonstrated potential for electronic applications in thin film form[15] has been grown as single crystals from the vapor phase, allowing comparison of technological and intrinsic properties of the material.

Experimental Section

Material Synthesis. DiF-TES ADT is synthesized as reported in ref.[17] Similar to other anthradithiophene derivatives, both the syn- and anti-isomers are present.[14,17] In short, thiophene 2,3-diacetal is lithiated at $T = -78$ °C, followed by treatment with N-fluorobenzenesulfonamide and acid hydrolysis to yield 5-fluorothiophene-2,3-dialdehyde. This dialdehyde is then condensed in ethanol with 0.5 equiv. of cyclohexane-1,4-dione under mild basic catalysis, to yield the corresponding difluoro anthradithiophenequinone. DiF-TES ADT is formed by the addition of lithiated triethylsilyl acetylene to the aforementioned quinone suspended in dry THF, followed by deoxygenative workup with acidic $SnCl_2$ upon complete dissolution of the quinone. The product is purified by chromatography on silica (hexanes solvent) followed by recrystallization from hexane. ^{1}H NMR (400 MHz, $CDCl_3$): δ 0.91 (q, $J = 7.7$ Hz, 12H), 1.24 (t, $J = 7.8$ Hz, 18H), 6.82 (s, 2H), 8.85 (s, 2H), 8.93 (s, 2H) ppm.

Crystal Growth. We have grown the crystals by using the PVT method.[18] Before the growth, we cleaned the tube with soap, acetone, and isopropyl-alcohol and heated it in argon flow to remove possible contamination solvents. No additional purification was applied to the starting material. We placed the powder in the hot part of the tube, and then heated it at the sublimation temperature, $T_S \approx 185$ °C. The platelet-shaped crystals are formed at about 10−15 cm from the powder, at $T \approx 130$ °C. Typical growth time is around 3 days. After the crystals are formed, we annealed them in the growth tube for 3 h at $T = 80$ °C to decrease the number of dislocations and the stress in the crystal.

AFM Measurements. We made measurements using a MFP-3D (Asylum Research) AFM in tapping mode.[19] AFM tips were treated with OTS to minimize adhesion between the crystal surface and the tip. We placed the crystals on an oxidized silicon substrate using the electrostatic transfer method described in the device fabrication section.

TEM Measurements. For the TEM measurements, crystals were removed from the growth tube, suspended in distilled water, and deposited onto freshly cleaved mica. After thermal evaporation of an overcoat of carbon, the sample was floated onto water and retrieved on copper TEM grids. Electron diffraction and diffraction-contrast images of the crystals were obtained at 120 kV, using a Phillips 400T, and recorded with an SIS Cantega 2K CCD camera.[19]

Device Fabrication. The field-effect transistors consisted of heavily doped ⟨100⟩ silicon that we used as the gate electrode, with 200 nm thermally grown SiO_2 used as gate insulator. The source and drain electrodes (5 nm Ti and 40 nm Au) were deposited by e-beam evaporation and patterned by photolithography and a lift-off process. We used warm acetone, isopropanol, followed by ultraviolet-ozone exposure to clean the wafers. The oxide was treated with octyltrichlorosilane (OTS) by immersing freshly cleaned wafers in a 8 mmol/L solution of OTS in anhydrous hexadecane for 1 h, followed by sonication in chloroform and isopropanol, consecutively.

We fabricated the single-crystal devices by placing the freshly grown crystals (having thickness between 0.5 and 1 μm) on top of the transistor structure as the last step of the process, by an electrostatic bonding technique (see the inset in Figure 3b).[20,21] This process took place in air.

(15) Gundlach, D. J.; Royer, J. E.; Park, S. K.; Subramanian, S.; Jurchescu, O. D.; Hamadani, B. H.; Moad, A. J.; Kline, R. J.; Teague, L. C.; Kirillov, O.; Richter, C. A.; Kushmerick, J. G.; Richter, L. J.; Parkin, S. R.; Jackson, T. N.; Anthony, J. E. *Nat. Mater.* **2008**, *6*, 216.
(16) Jurchescu, O. D.; Hamadani, B. H.; Xiong, H. D.; Park, S. K.; Subramanian, S.; Zimmerman, N. M.; Anthony, J. E.; Jackson, T. N.; Gundlach, D. J. *Appl. Phys. Lett.* **2008**, *92*, 132103.
(17) Subramanian, S.; Park, S. K.; Parkin, S. R.; Podzorov, V.; Jackson, T. N.; Anthony, J. E. *J. Am. Chem. Soc.* **2008**, *130*, 2706. [Convention specifies that triclinic unit-cell angles should be chosen to be either all acute or all obtuse. In equivalent cells, such angles are related by their supplement. Note here that beta is essentially 90°]
(18) Laudise, R. A.; Kloc, C.; Simpkins, P.; Siegrist, T. *J. Cryst. Growth* **1998**, *187*, 449.
(19) NIST disclaimer: Certain commercial equipment, instruments, or materials are identified in this paper to foster understanding. Such identification does not imply recommendation or endorsement by the National Institute of Standards and Technology, nor does it imply that the materials or equipment identified are necessarily the best available for this purpose.
(20) Takeya, J.; Goldmann, C.; Haas, S.; Pernstich, K. P.; Ketterer, B.; Batlogg, B. *J. Appl. Phys.* **2003**, *94*, 5800.
(21) de Boer, R. W. I.; Klapwijk, T. M.; Morpurgo, A. F. *Appl. Phys. Lett.* **2003**, *83*, 4345.

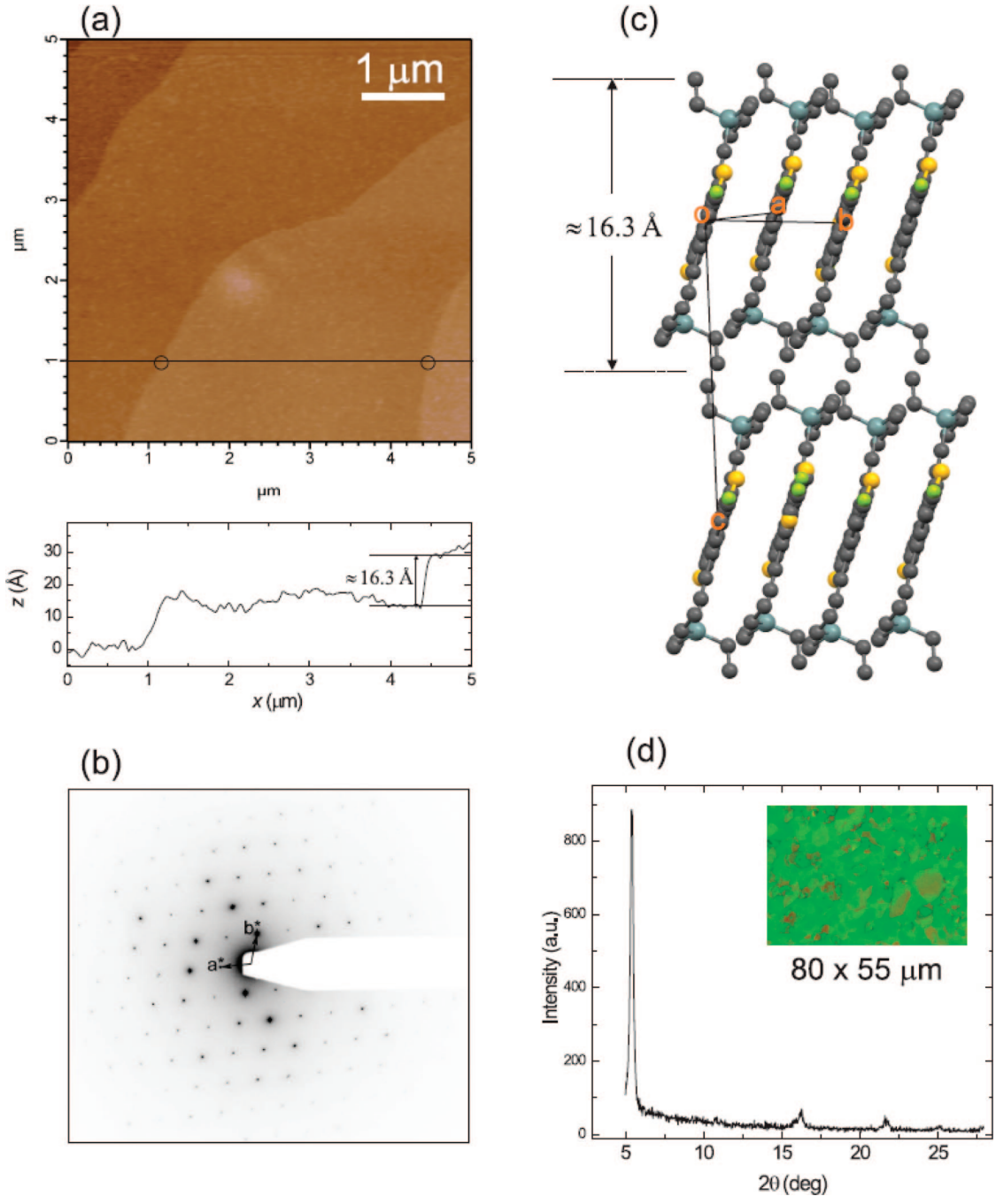

Figure 2. (a) Upper panel: AFM topography image of the surface of one diF-TES ADT single crystal showing characteristic steps. Lower panel: The step height represents the interlayer separation, $d = 16.3$ Å. (b) Electron diffraction (ED) pattern of a diF-TESADT single crystal at normal beam incidence. (c) DiF-TESADT crystal packing. The unit cell orientation is indicated. (d) $\theta-2\theta$ XRD results for a diF-TESADT film on a gold substrate, showing the preferential orientation. The inset shows an optical micrograph of the film taken by polarized light microscopy.

Results and Discussions

We used atomic force microscopy (AFM) and transmission electron microscopy (TEM) to characterize the surface topography and crystal orientation. The AFM images taken at the surface of the crystals, on a 5 μm × 5 μm area, show flat terraces parallel to each other (Figure 2a, upper panel). The surface of the crystal is smooth over large areas (more than 2 μm × 2 μm). This property is very important, as the transistor channel forms here, and the roughness, if present, will scatter the charges and decrease the mobility.[22]

The electron diffraction pattern in Figure 2b was obtained from a single crystal at normal beam incidence and demonstrates single-crystal order. The crystal structure is in agreement with the structure determined using X-ray diffraction (XRD) for single crystals obtained from solution:[17] triclinic symmetry, space group $P\bar{1}$ (unit-cell parameters: $a = 7.2089(10)$ Å, $b = 7.3170(11)$ Å, $c = 16.352(2)$ Å, $\alpha = 87.718(9)°$, $\beta = 89.993(9)°$, $\gamma = 71.940(8)°$). The crystal packing is shown in Figure 2c. The molecules are arranged in a layered fashion with a distance between the layers of 16.3 Å. Within the layers, the molecules adopt a 2D π-stack with the distance between molecular planes of ~3.4 Å. The analysis of this ED pattern demonstrates that the *ab* plane is

(22) Chua, L. L.; Ho, P. K. H.; Sirringhaus, H.; Friend, R. H. *Adv. Mater.* **2004**, *16*, 1609.

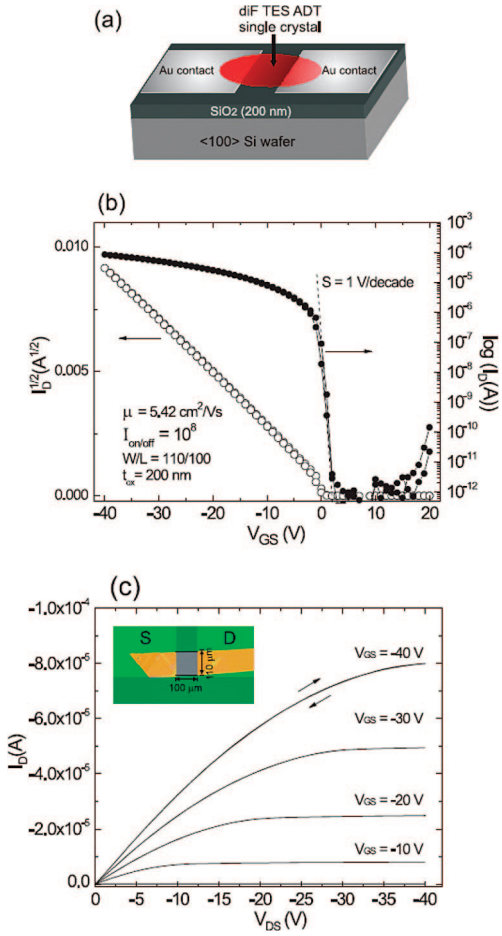

Figure 3. Electrical characteristics of a diF-TES ADT single crystal FET. (a) Schematic representation of the single-crystal FET. (b) Right axis: current−voltage characteristics ($\log(I_D)$ vs V_{GS}) at $V_{DS} = -40$ V. The geometry of the transistor is indicated. Left axis: $\sqrt{I_D}$ vs V_{GS} plot in the saturation regime. This yielded values of $\mu = 5.42$ cm^2/(V s) and $V_T = 2$ V. (c) Source-drain (I_D) current versus drain voltage (V_{SD}) recorded at different gate voltages (V_{GS}). The inset shows an optical microscope photo of a diF-TES ADT FET. The dimensions of channel length (L) and channel width (W) are indicated ($L = 100$ μm, $W = 110$ μm.).

essentially normal to the electron beam. The reciprocal lattice net exhibits the angle γ of approximately 71.9°. This conclusion is also supported by the value of step-height measured using AFM technique (Figure 2a, lower panel), which is consistent with the interlayer separation (Figure 2c) ($d_{001} = 16.3$ Å). The concurrence between the terrace height obtained by AFM and the interlayer separation extracted from TEM and XRD indicates that we are imaging the *ab* plane of the crystal.[2,23] This observation is important as this is the surface on which the field-effect transistor is fabricated. In the *ab* plane, the molecules present a cofacial orientation with respect to each other. This arrangement is predicted to be the most favorable stacking for charge transport.[7]

We show that our results obtained on vapor-deposited crystals have direct relevance to solution processing of a device. We have previously demonstrated that we can induce crystallinity in solution deposited diF-TES ADT devices using a very simple method of chemical modification of the contacts[15] (see the inset in Figure 2d showing an optical micrograph of the film under crossed polarizers). $\theta-2\theta$ X-ray diffraction (XRD) experiments performed on thin films deposited from solution on chemically modified Au (Figure 2d) demonstrate that the highly crystalline films have a preferred orientation, with the *ab* plane parallel to the substrate, similar to the single-crystal platelets. Because of this solution deposited film forming properties, diF-TES ADT is very different from other systems previously reported in literature. Rubrene, for example, exhibits a high mobility in the single crystal,[1] but a very low mobility when deposited from solution because the films are not crystalline.[24] On the other hand TIPS-pentacene shows higher mobility when deposited from solution[11] than in the evaporated films. We can only speculate that in the latter system, the reported differences in performance arise from thin film discontinuities or possible thermal decomposition of the material, or are a result of another crystal structure.[25] Unlike previously studied organic small molecules, in which dramatic differences were demonstrated between the performance of the single crystals and films,[24] with diF-TES ADT we see less than a 10× difference in mobility between solution deposited polycrystalline films and vapor-grown single crystals due to the high crystallinity of the solution-cast films.[15]

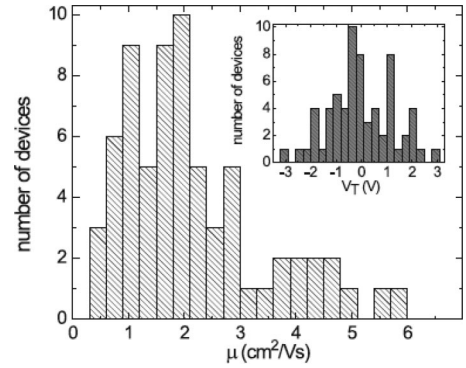

Figure 4. Histogram representing the values of mobilities (μ) measured for 68 diF-TES ADT single-crystal devices. The inset shows the spread in threshold voltage (V_T).

The schematic view of the single crystal transistor is shown in Figure 3a. All the electrical measurements were performed in a nitrogen purged probe station, at room temperature and in the dark. The device characteristics (mobility, hysteresis) vary from sample to sample, but this variation can be mitigated by applying an octyltrichlorosilane (OTS) treatment to the SiO_2 gate dielectric, yielding devices with consistently higher mobilities and much smaller hysteresis in current−voltage characteristics. Similar effects were observed by Goldmann et al. for devices fabricated using rubrene single crystals, where they estimated a reduction by a factor of 2 of the density of traps at the organic/dielectric interface when OTS treatment was used.[10]

(23) Menard, E.; Marchenko, A.; Podzorov, V.; Gershenson, M. E.; Fichou, D.; Rogers, J. A. *Adv. Mater.* **2006**, *18*, 1552.
(24) Stingelin-Stutzmann, N.; Smits, E.; Wondergem, H.; Tanase, C.; Blom, P.; Smith, P.; de Leeuw, D. *Nat. Mater.* **2005**, *4*, 601.
(25) Sheraw, C. D.; Jackson, T. N.; Eaton, D. L.; Anthony, J. E. *Adv. Mater.* **2003**, *15*, 2009.

Panels b and c in Figure 3 show plots of the transistor current−voltage characteristics of one of the single-crystal devices fabricated at the surface of OTS treated oxide that exhibited one of the highest mobilities, $\mu = 5.42$ cm^2/(V s). The graph in Figure 3b gives the log(I_D) vs V_{GS} (right axis) and $\sqrt{I_D}$ vs V_{GS} (left axis) plots in the saturation regime (drain-source voltage $V_{DS} = -40$ V) for a device with $W/L = 110\ \mu$m/100 μm, $t_{ox} = 200$ nm (see the inset of Figure 3c, showing the optical micrograph of the diF-TES ADT single crystal device (top-view)). We calculated the field effect mobility μ from the slope ($\partial\sqrt{I_D}/\partial V_{GS}$) of the$\sqrt{I_D}$ vs V_{GS} plots using the following expression

$$I_D = \frac{W}{L}\frac{C_i}{2}\mu(V_{GS} - V_T)^2 \quad (1)$$

where C_i is the gate oxide capacitance per unit area. The threshold voltage V_T, for this particular device, is $V_T = 2$ V. The small value of the threshold voltage, as well as the fact that the device shows almost no hysteresis between the forward and reverse sweeps, are good indications of a low trap density at the interface between the gate insulator and the organic semiconductor. This is also reflected in the small value of the subthreshold slope; for this particular device $S = 1$ V/dec. This value is comparable with the values obtained in rubrene and pentacene single crystal FETs, but in this case it is valid over a 5 orders of magnitude increase in current, compared to 3 orders of magnitude increase in current reported in ref 10. The very sharp turn-on in the weak accumulation region is particularly notable. This behavior is uncommon for most organic FETs reported to date, with the exception of a recent report on single-crystal FETs fabricated using Cytop[19] gate dielectric.[26] This property is important for low-power/low-voltage applications. The current on/off ratio is 1×10^8, which is typical for our diF-TESADT single-crystal FETs. Figure 3c shows the variation of the drain current (I_D) as a function of drain voltage (V_{DS}) for different gate voltages (V_{GS}). The increase in the current with increasing negative gate bias is consistent with the hole conduction expected for this material and contacts. The linear behavior at low V_{DS} and the absence of hysteresis between the forward and reverse bias sweeps indicates that device performance is not contact limited.

The histogram shown in Figure 4 gives an overview of the values of the field effect mobility (μ) measured on 68 single crystal devices. The crystals used for the fabrication of these devices are obtained from three different growth runs under argon flow. The channel length of these devices is $L = 80$ or 100 μm, and the channel width W is between 50 and 500 μm, given by the dimensions of the crystals. The minimum measured mobility is $\mu = 0.52$ cm^2/ Vs, and the maximum is $\mu = 6$ cm^2/ Vs, with 55 devices showing mobilities larger than 1 cm^2/ Vs. The spread in the calculated values of mobility is a consequence of the different crystal and contact qualities, errors in estimation of the transistor geometry (L and W), as well as perhaps anisotropy in mobility along the different crystallographic directions.[1,27] The inset in Figure 4 gives the values of the threshold voltages for all the devices measured, immediately after fabrication. These properties of the diF-TES ADT single crystals are stable when exposed to ambient air and light.

The electrical properties of the diF TES ADT devices are superior to those of thin film devices reported in refs 15 and 16 (sharper turn on, larger mobility and lower threshold voltage). The fabrication of FETs from vapor-grown crystals is expected to yield the ultimate performance of this class of materials and offers a test-platform for exploration of their intrinsic properties. The results presented here likely represent the lower limit of the material performance potential, as the fabrication of field-effect transistors based on diF-TES ADT single crystals is still in its infancy. With a better understanding of the material behavior under different conditions, and careful control during the different fabrication steps, one can further improve the performance of these single crystals and transfer the knowledge to the more technologically attractive solution-deposited films.

In conclusion, we have grown for the first time from vapor phase crystals of a solution processable oligomer that also exhibits promising properties in thin film form. Single crystal mobilities as high as $\mu = 6$ cm^2/ (V s), and I_{on}/I_{off} ratios of 1×10^8, subthreshold slopes of $S \approx 1$ V/dec, as well as low hysteresis in the transistor characteristics illustrate the technological potential of soluble oligomers and open new perspectives on the use of soluble organic semiconductors for high-performance electronic applications.

Acknowledgment. We acknowledge B. Hamadani and O. Kirillov for their assistance with the prefabricated substrates, and S. Parkin, C. Richter, L. Richter, and D. DeLongchamp for their insightful discussions during the preparation of the manuscript. J.E.A. and S.S. acknowledge the Office of Naval Research for support of the development of new organic semiconductors.

CM8021165

(26) Kalb, W. L.; Mathis, T.; Haas, S.; Stassen, A. F.; Batlogg, B. *Appl. Phys. Lett.* **2007**, *90*, 092104.

(27) de Wijs, G. A.; Mattheus, C. C.; de Groot, R. A.; Palstra, T. T. M. *Synth. Met.* **2003**, *139*, 109.